Numerical Simulation of load/unload in small form factor hard disk drives

P. Bhargava and D. B. Bogy
Computer Mechanics Laboratory
Department of Mechanical Engineering
University of California
Berkeley, CA 94720

Abstract

Over the past decade, there has been a substantial transition from contact start stop (CSS) technology in hard disk drives (HDD) to the more advanced load unload (L/UL) technology. L/UL offers many advantages over CSS, such as a cure for stiction and reduced wear. In this report we present a procedure for simulating the load/unload process in a HDD. A coupled structural-fluid model is presented which can be used to obtain the dynamic response of the slider-suspension-disk system. The model is based on the CML dynamic air bearing code. This simulator offers many advantages over the prior CML 4-DOF L/UL simulator developed earlier [1], with only minor increase in the computation times. Some of these advantages are the modeling of actuator rotation, shear force inclusion, dimple, limiter and ramp impact modeling and user defined ramp profiles. Using the new simulator we simulate loading and unloading processes for a 1" drive and compare the results to those obtained using the former CML 4-DOF L/UL simulator. We find that the FE model based simulator is in excellent agreement with the 4-DOF simulator for unloading. We also find good agreement between the two simulators for slow loading processes. However, for faster loading processes the results are different. We have tried to explain the differences on the basis of 'false effective mass' of the 4-DOF simulator during multiple suspension states. We also compare the results in the frequency domain and observe certain additional improvements over the 4-DOF simulator.

1 Introduction

Load/Unload (L/UL) technology today has widespread application in small form factor drives. Although the first application of load/unload technology was as early as the late 1950s the ramp load/unload technology of today first appeared in mobile drives in the early 1990s. The ramp load/unload system is now well established as the standard for almost all segments of small form factor drives: from 2.5" mobile drives to the 1"-0.8" drives, which today find widespread application in a host of consumer electronic devices.

Load/unload technology offers many advantages over the traditional contact start stop (CSS) technology. One of the most important advantages is the much greater shock resistance in the non-operational state. Today's drives equipped with L/UL systems can withstand shocks, which would fatally damage the air-bearing slider and the disk in CSS systems. And with the emergence of smaller form factor drives such as, the 1" and the 0.8" drives which find widespread application in shock-prone environments like MP3 players and cameras, shock resistance is perhaps the biggest boon of L/UL technology. A shock simulation study using a somewhat different simulator was presented in [2].

Another advantage of L/UL is that of avoiding the problem of stiction, which CSS systems are inherently prone to. This leads to lower power consumption as well as lower wear and debris for the ABS.

L/UL technology also has the potential to do away with CSS landing zones, and with efforts being made to load/unload on data tracks, this valuable space on the disk can be recovered to increase the storage capacity of the drive.

The main design objectives of L/UL are to avoid or at least minimize the occurrence of slider-disk contacts leading to media and head damage, small ramp forces such that ramp wear is minimized, and a smooth and short unloading process. In the period from 1988 to

2003, many pioneering studies [1, 3-6, 9-13] on L/UL were carried out at the Computer Mechanics Laboratory (CML) at U.C. Berkeley.

It is found that the suspension model is critical in the simulations. The 4-DOF suspension model proposed by Zeng et al [1] was perhaps the most accurate L/UL model previously developed. However in this paper we present a new and improved L/UL simulator with more sophisticated and complete modeling for the suspension. We incorporate FE modeling for the suspension for simulating load/unload by incorporating pre-assembled mass and stiffness matrices for the suspension into the CML L/UL Simulator. The new simulator allows us to model the actuator swinging motion during the load and unload processes so that these processes can be more realistically simulated. This new simulator also allows us to simulate the loading and unloading processes much more accurately without any significant loss in computational efficiency as compared to the simulator developed in [1]. There are several additional improvements, such as inclusion of shear forces for the air bearing, direct use of a user-defined variable ramp profile and also modeling of shock (refer to [2]) during load/unload. The simulator developed here is different from that in [2] in that here we avoid the need to run ANSYS in parallel with the air bearing simulator by doing suspension calculations within the dynamic simulator itself. In this paper we present some results from this new simulator and compare these results with those predicted by the previous L/UL Simulator developed at CML [1].

2 Simulation Procedure

The simulation procedure for L/UL is based on two modules that perform the suspension modeling and the air bearing modeling. The loading and unloading processes are determined by the suspension dynamics as well as the air bearing forces. The suspension dynamics equations are solved using the finite element method. The generalized Reynolds equation for the air bearing is solved using the finite volume method. Contacts

between the slider and the disk are modeled using the Greenwood-Williamson statistical elastic asperity model. The solver for each component is integrated into the CML Load/Unload Simulator.

2.1 Suspension modeling

Figure 1 shows a finite element model of the suspension used in a currently popular 1" drive (figure 3). A schematic of the suspension with various components labeled is shown in figure 2. The model was created in ANSYS, which is a widely used commercial finite element package. For simulating load and unload, we know there are only small displacements and the behavior of the suspension is linear except for the contacts at the dimple and limiters. Our procedure involves integrating mass and stiffness quantities over the elements as well as assembling the global stiffness and mass matrices in ANSYS and then exporting these matrices for use within the CML L/UL simulator. However this particular suspension model and suspension models in general are very complex and require a very large number of degrees of freedom, often of the order of a few hundred thousand. Since using such a large number of degrees of freedom for modeling the dynamics of the suspension would be severe overkill, we employ a method called dynamic reduction (also known as Guyan reduction or substructuring in ANSYS) to reduce the degrees of freedom to a more manageable number (of the order of several hundred). The resulting matrices are imported into the CML L/UL simulator and the nonlinearity of the contact elements is incorporated by imposing external contact element constraints on the pre-assembled matrices.

2.2 Air bearing modeling

The air bearing modeling is done using Patankar's finite volume method. This procedure has been documented in detail in several CML reports [14]. However in addition, 6

degrees of freedom (DOF) are used here to model the slider state: the displacements and rotations in each of the 3 directions (x, y and z).

2.3 Coupling

The structural and air bearing components are coupled by a fixed point iteration scheme that iterates all forces and displacements at each time step to convergence. The basic scheme is shown in figure 4.

3 Simulation results

Simulations were carried out for two loading and unloading processes, and the results were compared with those of the previous version of the CML L/UL simulator. The simulations were carried using a slider from a currently popular 1" drive shown in figure 5. The operation parameters for this slider suspension system are listed in table 1. The new simulator models actuator rotation over a user defined ramp profile. However since the 4-DOF model simulator models the loading and unloading processes as a constant velocity load and unload, a flat ramp profile of inclination 27.7 degrees was used here in the new simulator for compassion of the two simulators. Also the loading and unloading processes were coupled with a track seek motion in the 4-DOF simulator to model the effect of the actuator motion.

3.1 Unloading process

The unloading process was simulated using the new as well as the previous versions of the CML L/UL simulators.

The first unloading process simulated was for a vertical unloading velocity of 44.44 mm/s (this corresponds to turning the actuator at a constant angular velocity of 4 rad/s). The simulation results are plotted in figures 6-9. Figure 6 has several plots showing various

components of the attitude of the slider for the two simulators; the slider center displacements in a), the nominal fly heights in b), the minimum clearances in c) and the rolls and the pitches in figures d) and e) respectively. We see that the unloading results predicted by the two simulators are very similar, with both the simulators predicting that unloading occurs at about 3.1 ms. However, we notice that more suspension oscillations as well as lesser damping is predicted by the FE model based simulator (using similar damping parameters), especially in the z and the pitch directions. Figure 7 plots the forces during the unloading process. The force curves show remarkable agreement, with both the simulators predicting slider disk impact at about 2.5 ms and 3 ms. In figure 8 we plot the ramp and the tab positions in a) and ramp contact forces for both of the simulators in b). We see that the ramp contact forces follow the same trend in the two simulations, however, in the FE based simulator we see a much richer frequency content as well as the effect of oscillations during the unloading process. In figure 9, we plot the status of the contact elements in the FE based simulator, which gives us information regarding the dimple contact forces and the limiter forces. In a), we can see how the dimple separates and following the unloading process, how the flexure oscillates and impacts the load beam. These contact forces are plotted in b), where we see that the maximum magnitude of these forces exceeds 60 mN, which would likely lead to wear of the dimple and also generate debris inside the drive. In c) and d) we see that the limiters do not engage during this particular unloading process. The two curves correspond to the two contact elements on both sides of the hammer head limiter. This data is not compared to the 4-DOF based simulator, since that simulator is unable to generate these results.

The second unloading simulation was for an unloading velocity of 88.89 mm/s, achieved by doubling the angular velocity of the actuator to 8 rad/s. The slider attitudes for this process are plotted in figure 10. Again the results from the two simulators are in good agreement. Figure 11 plots the forces for the second unloading process. The forces are in

good agreement, however there is a slight difference after about 1.8 ms, which is the time when the limiters engage. This difference can be attributed to the fact that the new simulator describes the actual impact between the limiters and the load beam using contact elements rather than modeling the limiter engagement solely as a change in stiffness of the suspension. In figure 12 a) we again plot the ramp and tab positions as a function of time. In b) we plot a comparison of the ramp forces. The results are similar to those discussed for the previous unloading process. In figure 13, we plot the contact element behavior. Subplots a) and b) show the dimple spacing and contact forces. Here we see that the contact forces at the dimple exceed 80 mN, which may be harmful for the drive in terms of particle contamination. In c) we plot the limiter spacing, where we see that the limiter closes at about 2 ms, after which the slider quickly unloads from the disk.

3.2 Loading process

The loading process was first simulated using a vertical loading velocity of 50 mm/s. The results for the comparison of this loading process between the two simulators are plotted in figures (14-17). Figure 14 plots the slider attitude as predicted by the two simulators. The various quantities plotted are the slider centre displacements in a), the nominal fly heights in b), minimum clearances in c) and rolls and pitches in d) and e) respectively. We see that the HGA moves down the ramp, and the slider reaches the disk at about 3 ms. We see in figure 15 that the processes predicted by the two simulators are qualitatively and quantitatively very similar in the slider behavior as well as the development of the air bearing. There are no impacts during the loading process and the magnitudes of the asperity contact forces are also almost the same. In figure 16, we plot the ramp and tab positions in a) as well as the ramp contact forces in b). In figure 17, we plot the contact element data. In a) we see that the dimple is initially in the open position. This is because even though there is a dimple preload, the bending of the load beam due to the ramp

negates the effect of the preload in the parked state. During the course of the loading process, oscillations cause the flexure to strike the load beam until it finally closes at about 2.4 ms as the slider begins to load onto the disk through the air bearing.

For the second loading simulation case, we increase the loading velocity to 66.67 mm/s, using the same ramp profile, but increasing the actuator angular velocity to 8 rad/s. Again we observe that the attitudes predicted by the two simulators, as plotted in figure 18, are quite similar. In this case, however we see that the 4-DOF model predicts slider disk impact at about 2.5 ms. In c) in the inset zoomed plot, we can see that there is an impact at about 2.5 ms. Also since the pitch is negative, it is the front of the slider which hits the disk. This can also be seen from the force plots in figure 19. In c) we see an impact between the slider and the disk at about 2.5 ms when the air bearing has not yet fully developed. This seems to be the result of strong oscillations of the slider in the pitch direction. In the 4-DOF model based simulator, all of the suspension mass is transferred to the slider as the 'effective mass' of the slider. Hence the slider has the same 'effective mass' irrespective of whether the dimple is closed or open, whereas in reality this would depend on whether the dimple is closed or open. Thus we see that when the dimple closes during the loading process at ~2 ms as seen in figure 21, the magnitude of the pitch oscillations reduces as some of the energy is transferred to the load beam for the FE model based simulator, whereas for the 4-DOF simulator, the oscillation magnitude remains the same. This leads to the slider-disk impact.

Increasing the loading speed, we observe similar behavior with the 4-DOF model based simulator, predicting contacts which may not have occurred.

3.3 Frequency content

Figure 22 compares the frequency contents between the two simulators for a typical loading process. In a), b) and c), we plot the spectra for the 4-DOF based simulator and in

d), e) and f), we plot the spectra for the FE based simulator. In a) we observe two distinct peaks labeled 1 and 2. Peak 1 corresponds to the first bending mode of the suspension at 320 Hz, which was used to calculate the 'effective mass' of the slider in the 4-DOF suspension model. The second peak, at about 800 Hz, corresponds to the bending frequency of the system when the dimple is open. Since the 'effective mass' of the slider is unchanged in this state, this is actually a 'false' frequency, a figment of the mathematical modeling. In b) which plots the pitch curve, we again see these two frequency peaks. In c) where the roll frequency is plotted we again observe the false frequency at 800 Hz, which is seen in roll as a result of the coupling between roll and bending (since the stiffness matrix is not diagonal). We also observe a sharp peak 3 at ~2700 Hz which corresponds to the first torsion mode of the suspension, which was used to calculate the effective mass in the roll direction in the 4-DOF model.

For the FE-model based simulator, we observe much richer frequency spectra, as well as no false frequencies. In d), we observe various peaks labeled 1, 2, 3, 4 and 5 which correspond to the first bending (320 Hz), two flexure bending modes (dimple open, 1160 Hz), flexure bending mode (dimple closed, 1700 Hz), a third flexure bending mode (dimple open, 2100 Hz) and two flexure-load beam coupled bending modes (dimple open, 3220 Hz and 3180 Hz dimple closed). In e) which plots the pitch frequency, we see peaks 1,2,4,5 and in addition peaks 6 and 7 which correspond to a bending-torsion coupled mode (4056 Hz) and a load beam-second bending torsion coupled mode of the suspension (5900 Hz). For the roll, plotted in f), we observe peaks at 8, 6 and 9. Here 8 is the first torsion mode (2700 Hz) of the suspension.

4 Conclusion

We developed a new load/unload simulator based on finite element modeling of the suspension. We compared simulation results obtained using the new simulator with those

based on the CML 4-DOF model for two loading and unloading cases. We found that the results are in excellent agreement for unloading and for the slower loading processes. However for faster loading processes, we found slider-disk contacts in results obtained using the 4-DOF simulator which were not predicted by the FE based simulator. We explained these false contacts as being a result of by the same 'effective mass' being used for the suspension for all suspension states. Finally we also compared the spectra of various parameters and found the existence of false frequencies in the 4-DOF based simulator as well as a much richer modal representation for the FE model based simulator. This makes the FE based L/UL simulator much more useful in the simulation of faster loading and unloading processes in the presence of strong disturbances as well as other phenomena such as shock and vibration.

References

[1] Zeng, Q. and Bogy, D. B., 1999, "A Simplified 4-DOF Suspension Model for Dynamic Load/Unload Simulation and Its Application", Technical Report No 1999-003, Computer Mechanics Lab, Department of Mechanical Engineering, University of California, Berkeley.

[2] Bhargava, P. and Bogy, D. B., 2005, "Numerical Simulation of Operational-Shock in small form factor drives" , Technical Report No 2005-005, Computer Mechanics Lab, Department of Mechanical Engineering, University of California, Berkeley.

[3] T. G. Jeong, and D. B. Bogy, "Numerical Simulation of Dynamic Loading in Hard Disk Drives," ASME Journal of Trib., Vol. 115, 370-375, 1993.

[4] Zeng, Q. and Bogy, D. B., 1999, "Effects of Suspension Limiters on the Dynamic Load/Unload Process: Numerical Simulation", Technical Report No 1999-002, Computer Mechanics Lab, Department of Mechanical Engineering, University of California, Berkeley.

[5] Zeng, Q. and Bogy, D. B., 1998, "Slider air-bearing designs for load/unload applications", Technical Report No 1998-009, Computer Mechanics Lab, Department of Mechanical Engineering, University of California, Berkeley.

[6] Zeng, Q. and Bogy, D. B., 1999, "Effects of Certain Design Parameters on Load/Unload Performance", Technical Report No 1999-010, Computer Mechanics Lab, Department of Mechanical Engineering, University of California, Berkeley.

[7] Suk, M. and Albrecht, T. R., "The evolution of load/unload technology", Microsystem Technologies 8 10-16, Springer-Verlag, 2002.

[8] Albrecht, T.R. and Sai, F., "Load/Unload technology for disk drives", IEEE Trans. Magn., Vol. 35, pp. 857-862, 1999.

[9] Chapin, M. and Bogy, D. B., 1999, "Air Bearing Force Measurements of Pico Negative Pressure Sliders During Dynamic Unload", Technical Report No 1998-001, Computer Mechanics Lab, Department of Mechanical Engineering, University of California, Berkeley.

[10] Q. H. Zeng, M. Chapin and D. B. Bogy, "Dynamics of the unload process for negative pressure sliders," IEEE Trans. Magn., Vol. 35, pp. 916-920, 1999.

[11] Jeong, T.G. and Bogy, D. B., "Slider disk interactions during the load-unload process", IEEE Trans. Magn., Vol. 26, pp. 2490-2492, 1990.

[12] Jeong, T.G. and Bogy, D. B., "Measurements of slider-disk contacts during dynamics load-unload", IEEE Trans. Magn., Vol. 27, pp. 5073-5075, 1991.

[13] Yamada, T. and Bogy, D. B., "Load Unload slider dynamics in magnetic disk drives", IEEE Trans. Magn., Vol. 24, pp. 2742-2744, 1988.

[14] Lu, S., 1997, "Numerical Simulation of Slider Air Bearings", PhD Thesis, University of California, Berkeley.

Drive form factor	1”
Gram load	1.25 g
RPM	3600
Steady state FH	5.5 nm
Steady state Pitch	95 µrad
Steady state Roll	-5 µrad

Table 1. ABS Parameters

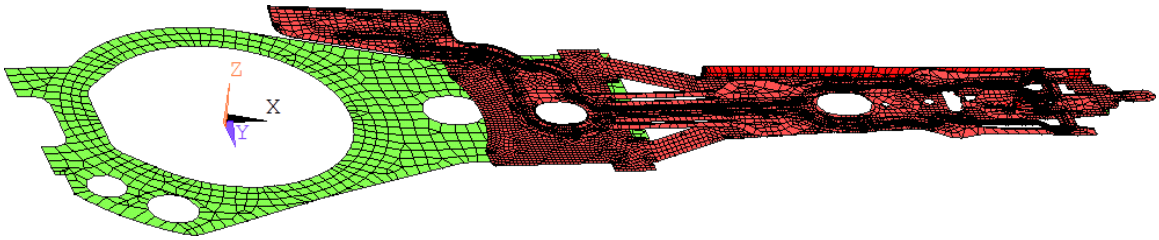

Fig 1. Suspension model

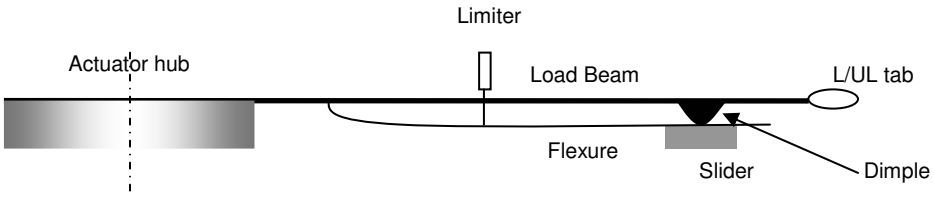

Fig 2. Suspension schematic

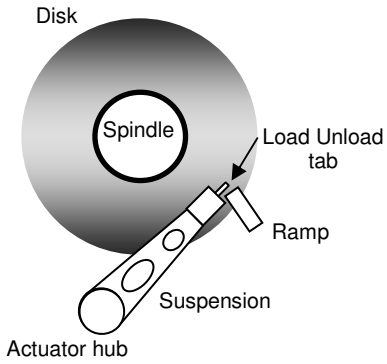

Fig 3. 1” drive schematic

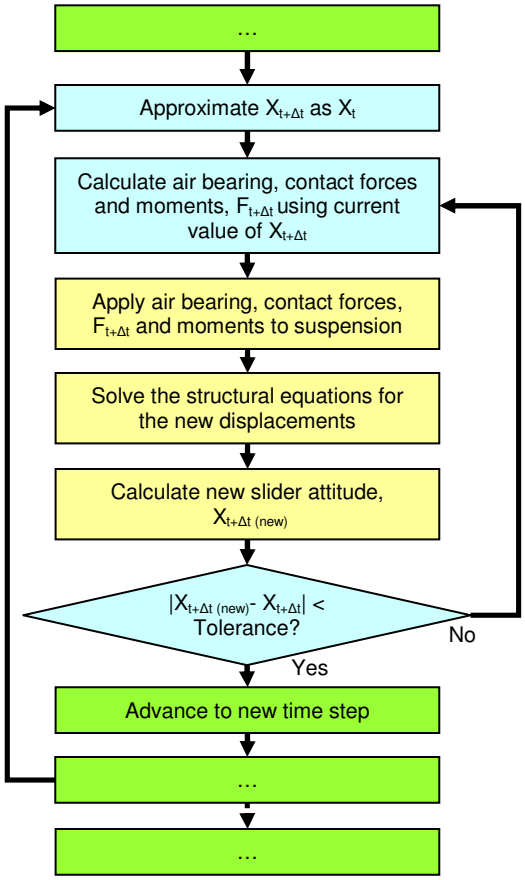

Fig 4. Structural-Air bearing coupling scheme

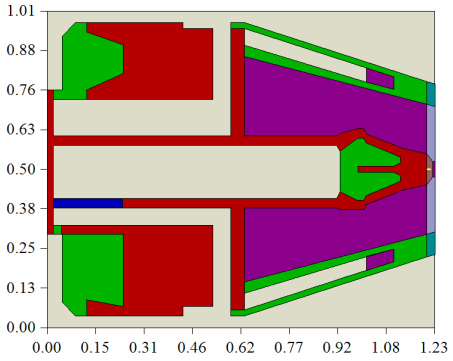

Fig 5. ABS Design

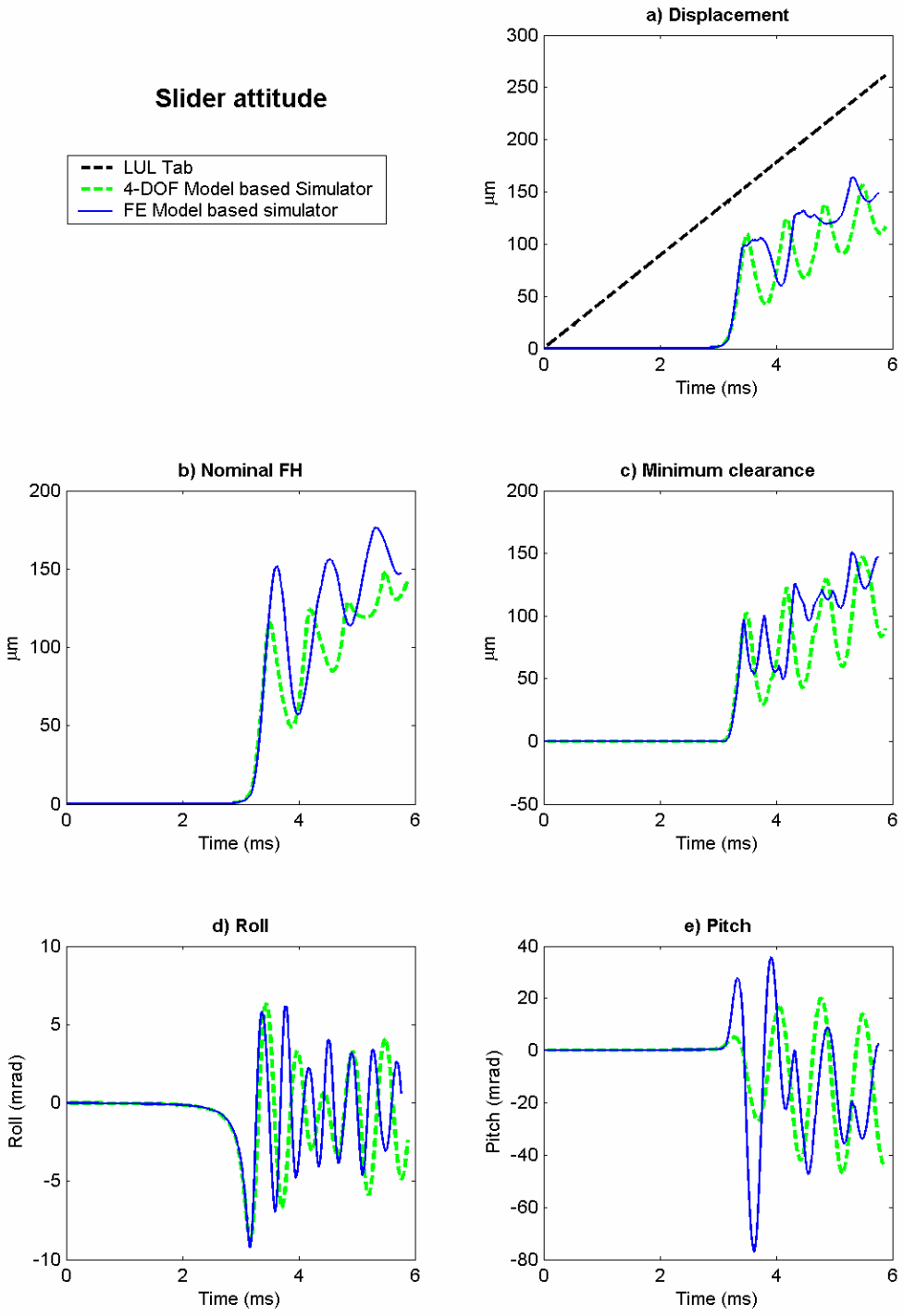

Fig 6. Slider attitude history comparison during the unloading process (44.4 mm/s)

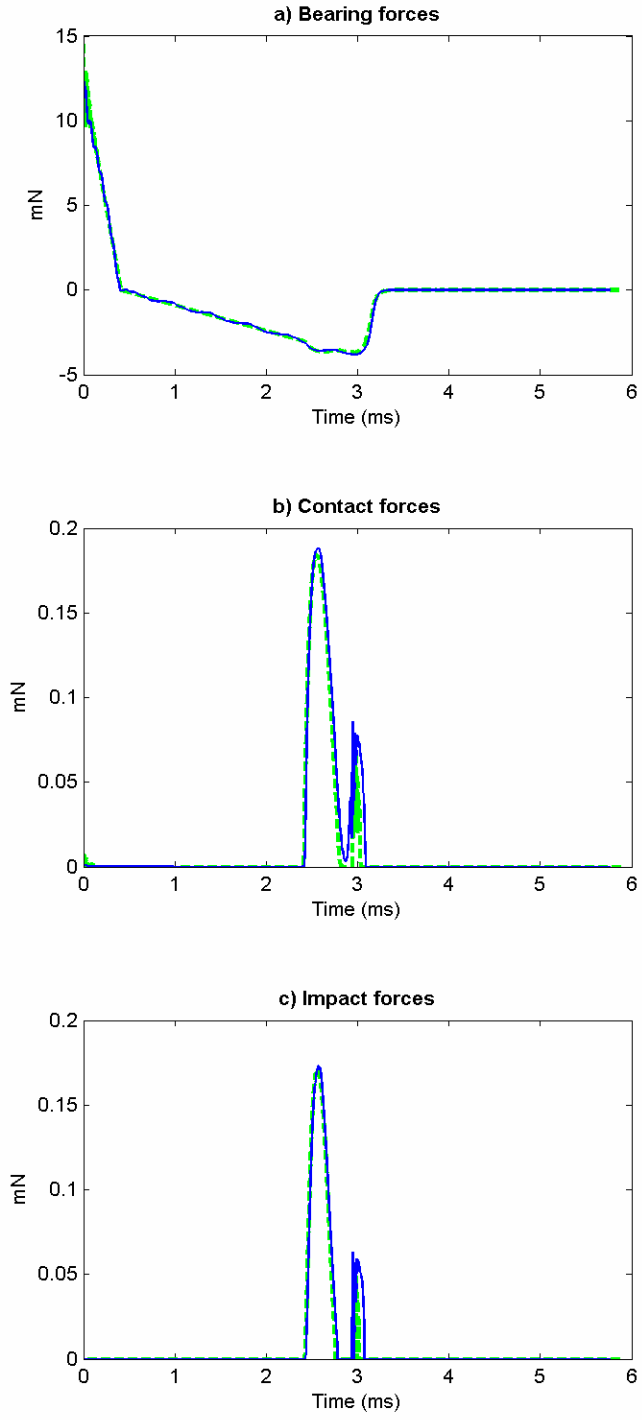

Fig 7. Force history comparison during the unloading process (44.4 mm/s)

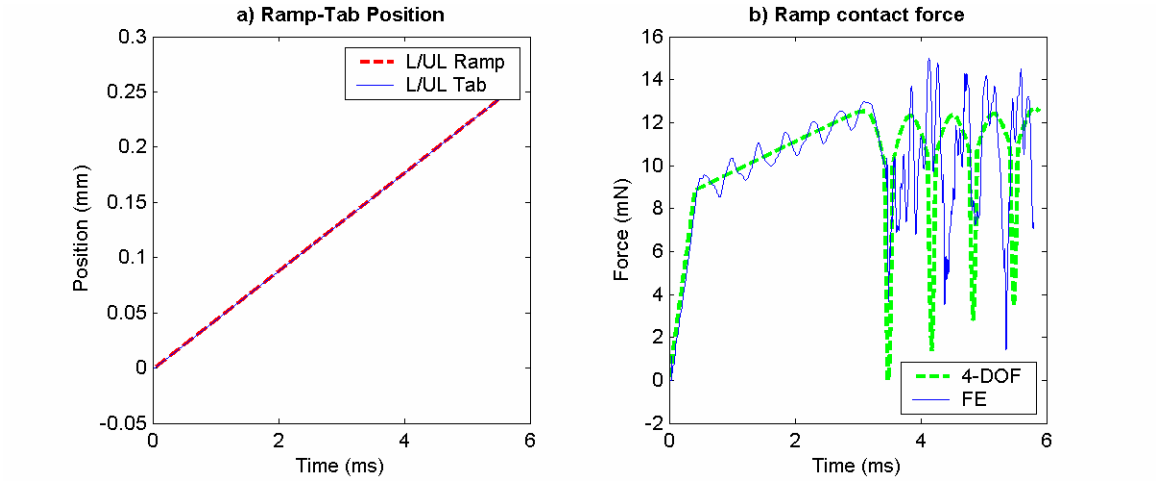

Fig 8. Ramp-tab position and ramp contact force during the loading process (44.4 mm/s)

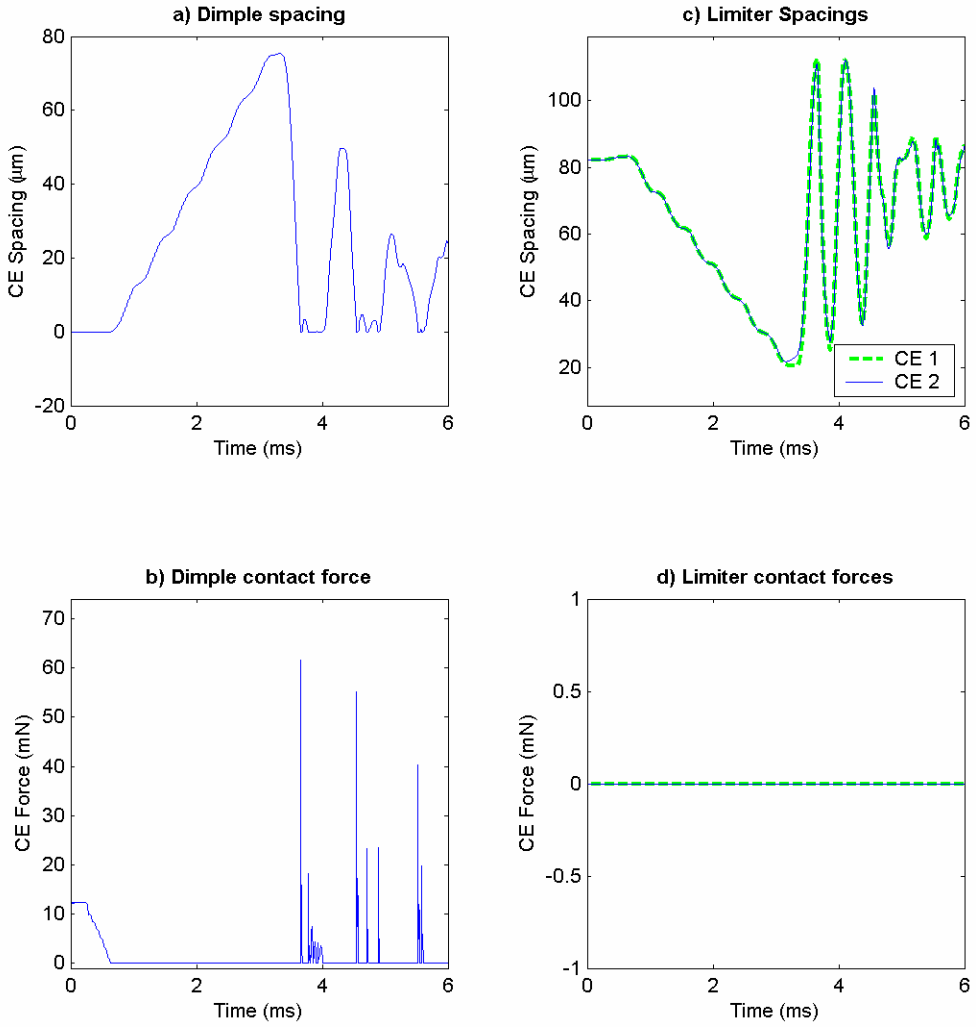

Fig 9. Dimple and limiter contact status during the loading process (44.4 mm/s)

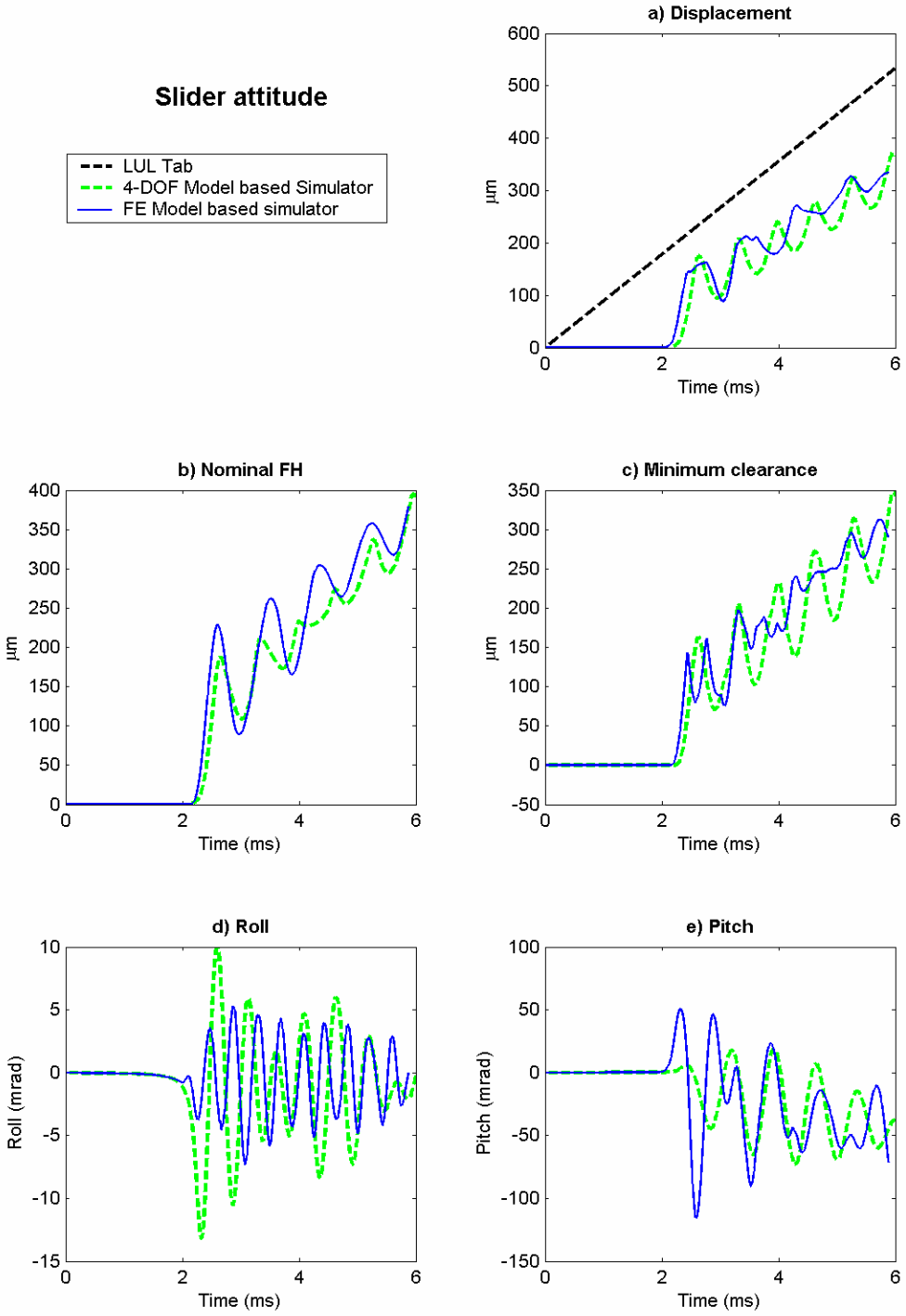

Fig 10. Slider attitude history comparison during the loading process (88.9 mm/s)

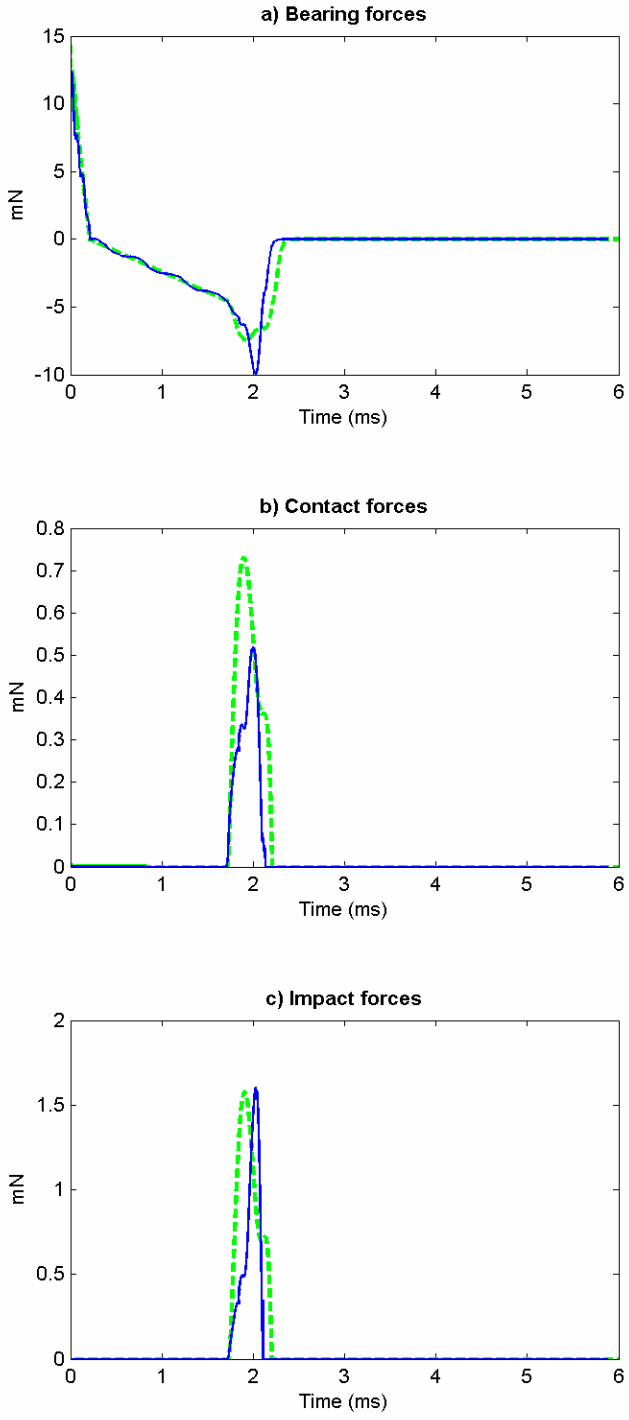

Fig 11. Force history comparison during the unloading process (88.9 mm/s)

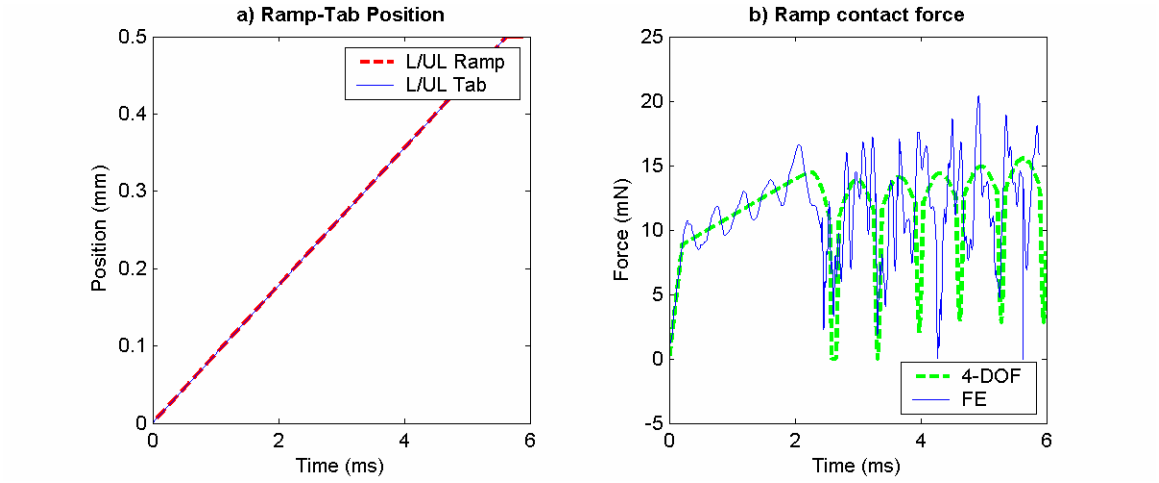

Fig 12. Ramp-tab position and ramp contact force during the loading process (88.9 mm/s)

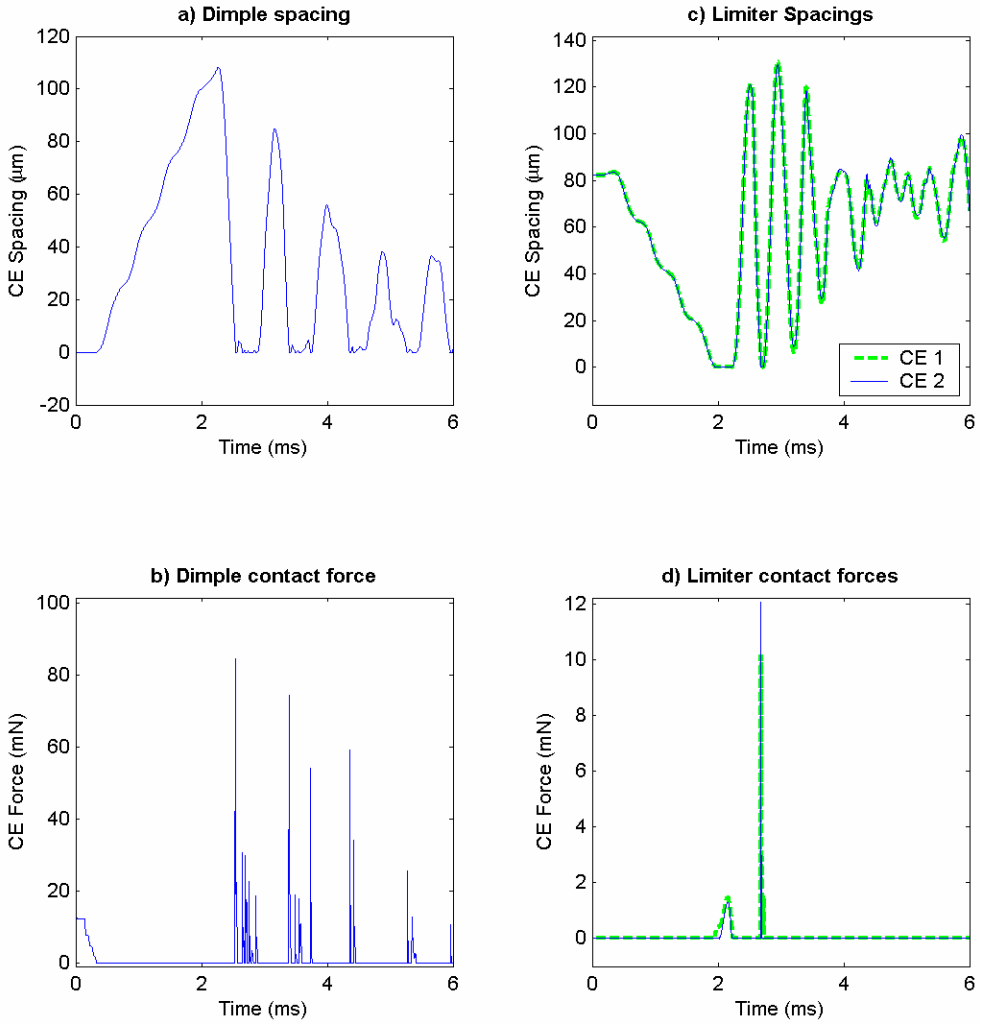

Fig 13. Dimple and limiter contact status during the loading process (88.9 mm/s)

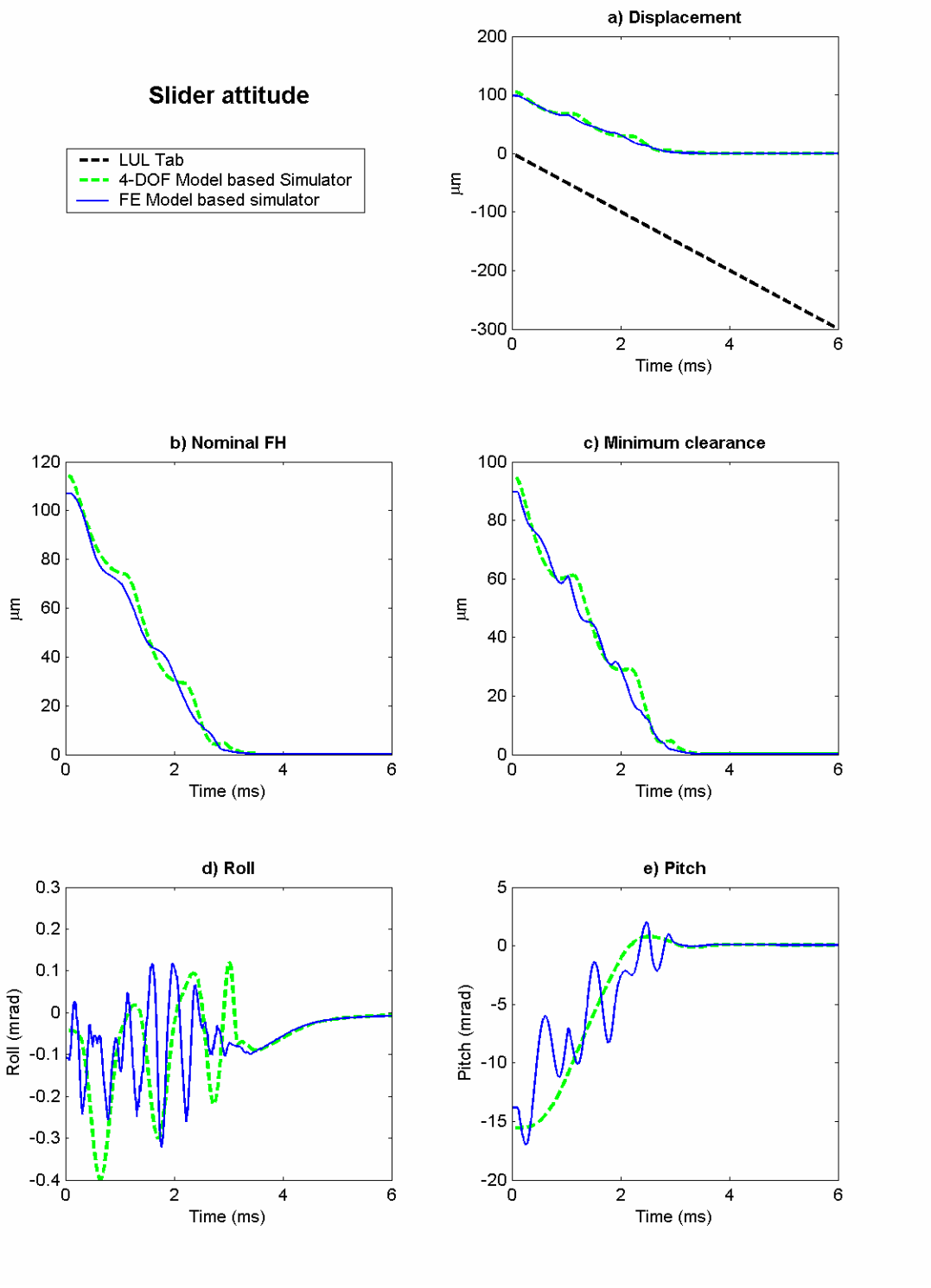

Fig 14. Slider attitude history comparison during the loading process (50 mm/s)

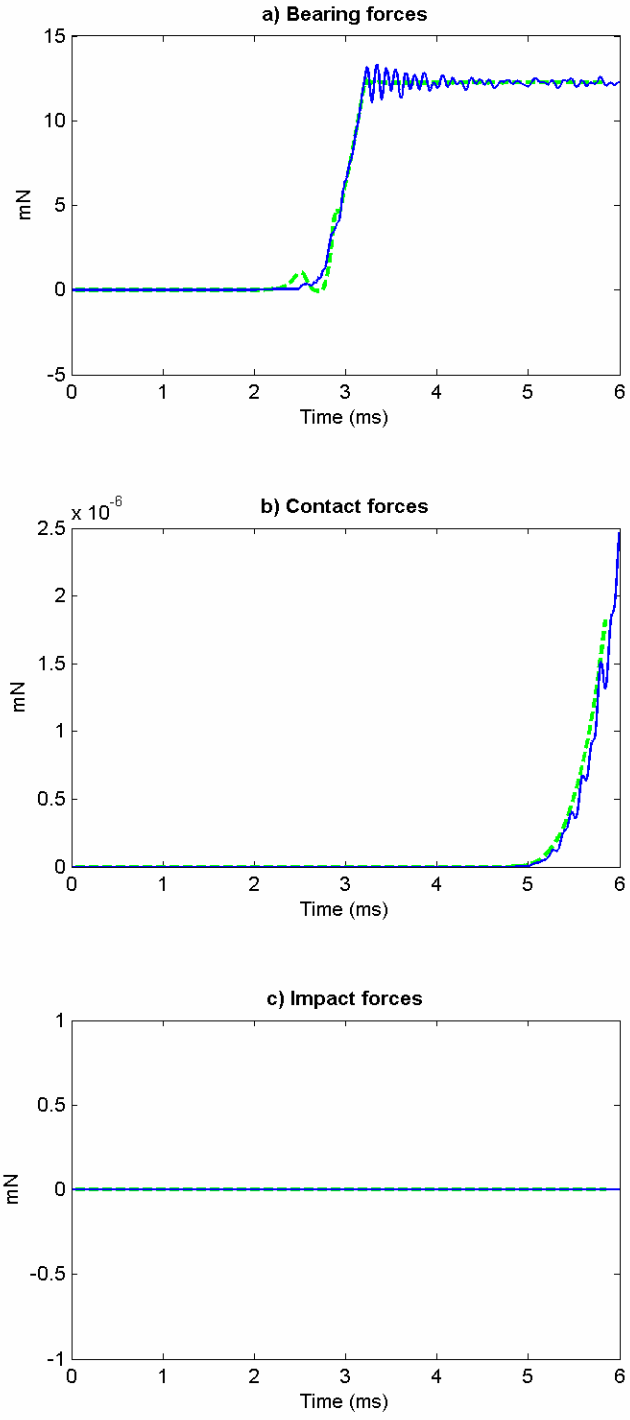

Fig 15. Force history comparison during the loading process (50 mm/s)

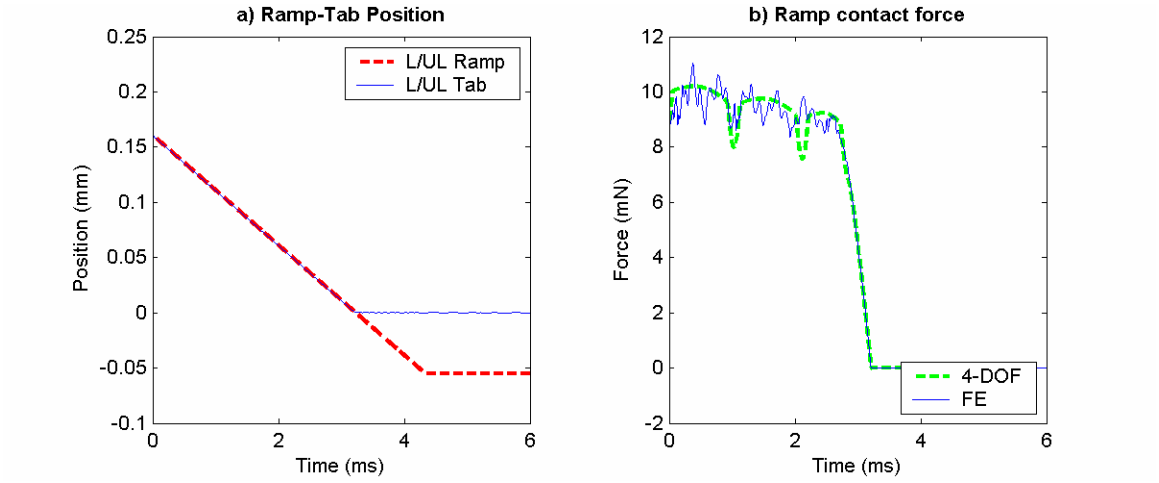

Fig 16. Ramp-tab position and ramp contact force during the loading process (50 mm/s)

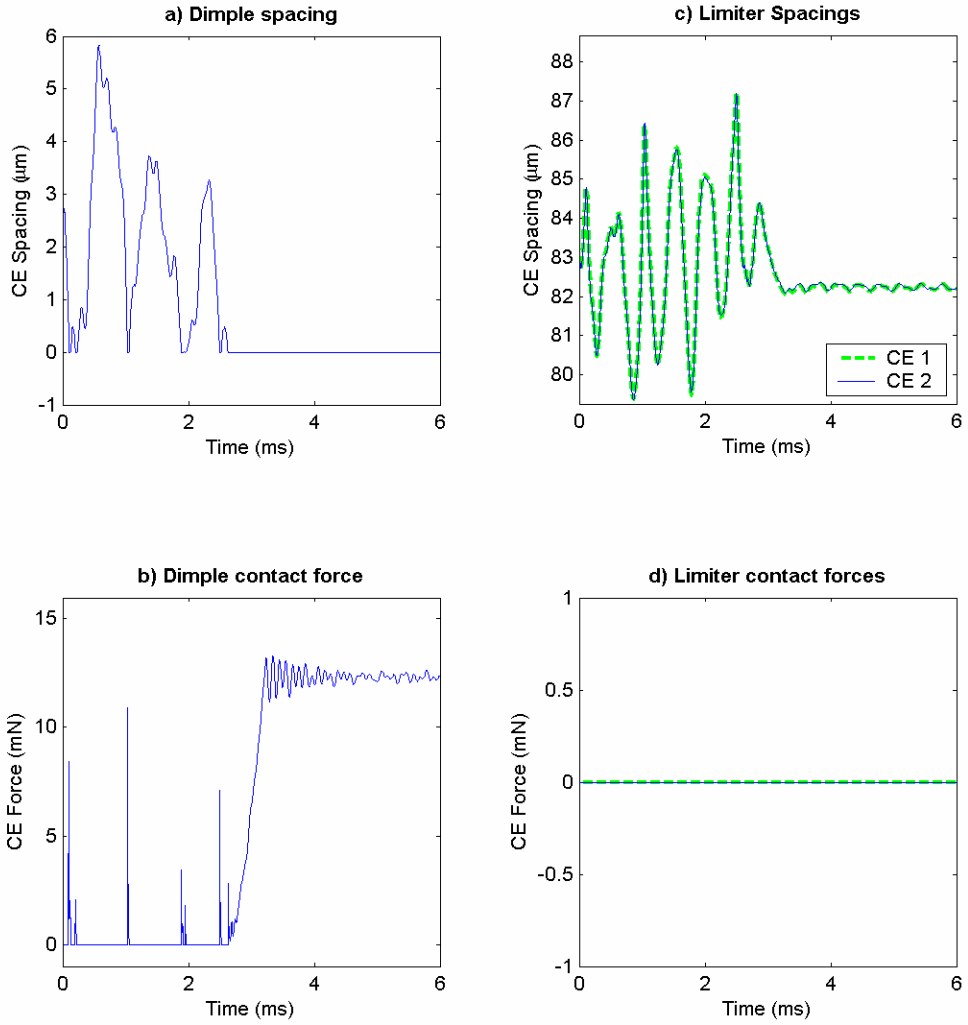

Fig 17. Dimple and limiter contact status during the loading process (50 mm/s)

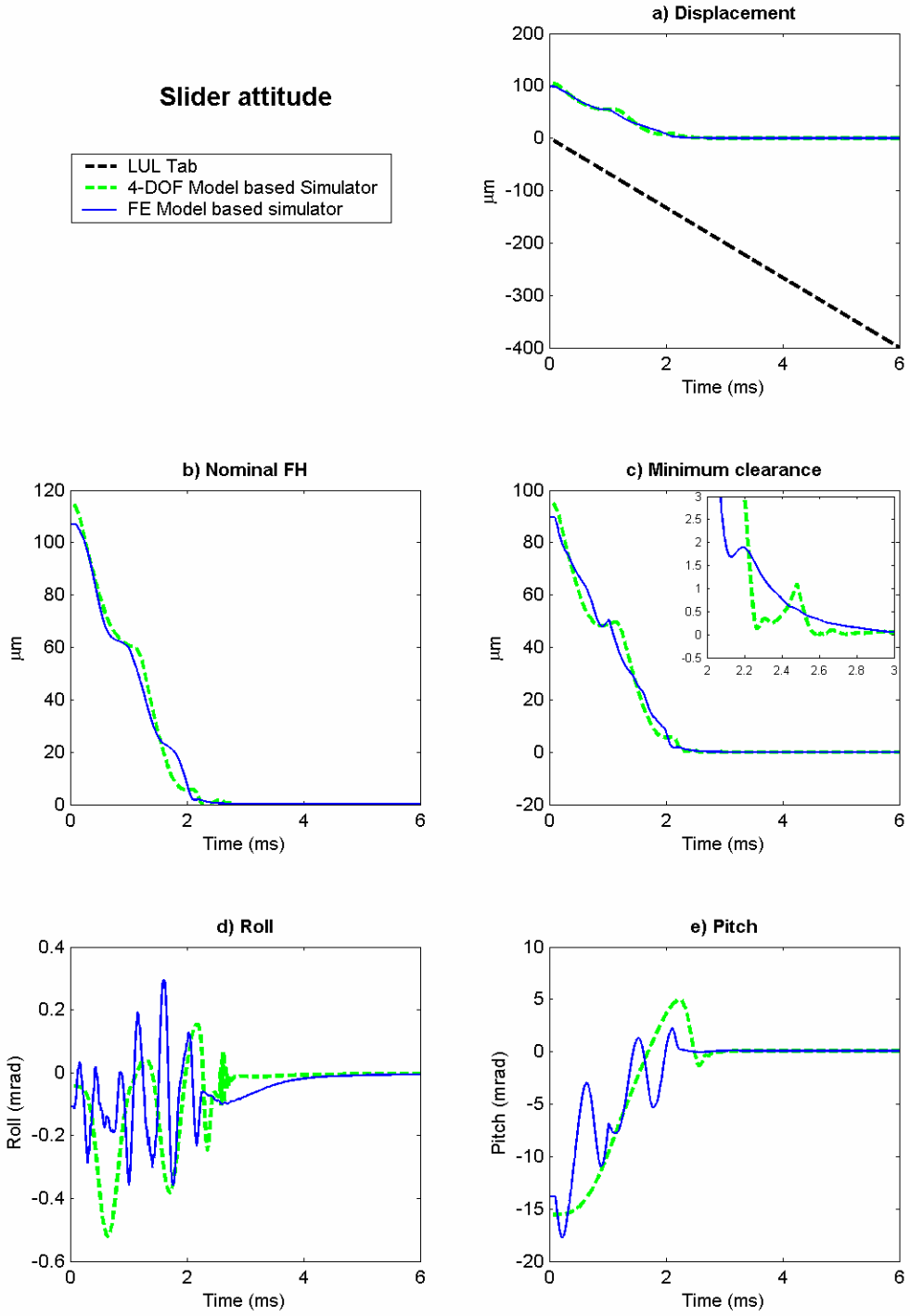

Fig 18. Slider attitude history comparison during the loading process (66.7 mm/s)

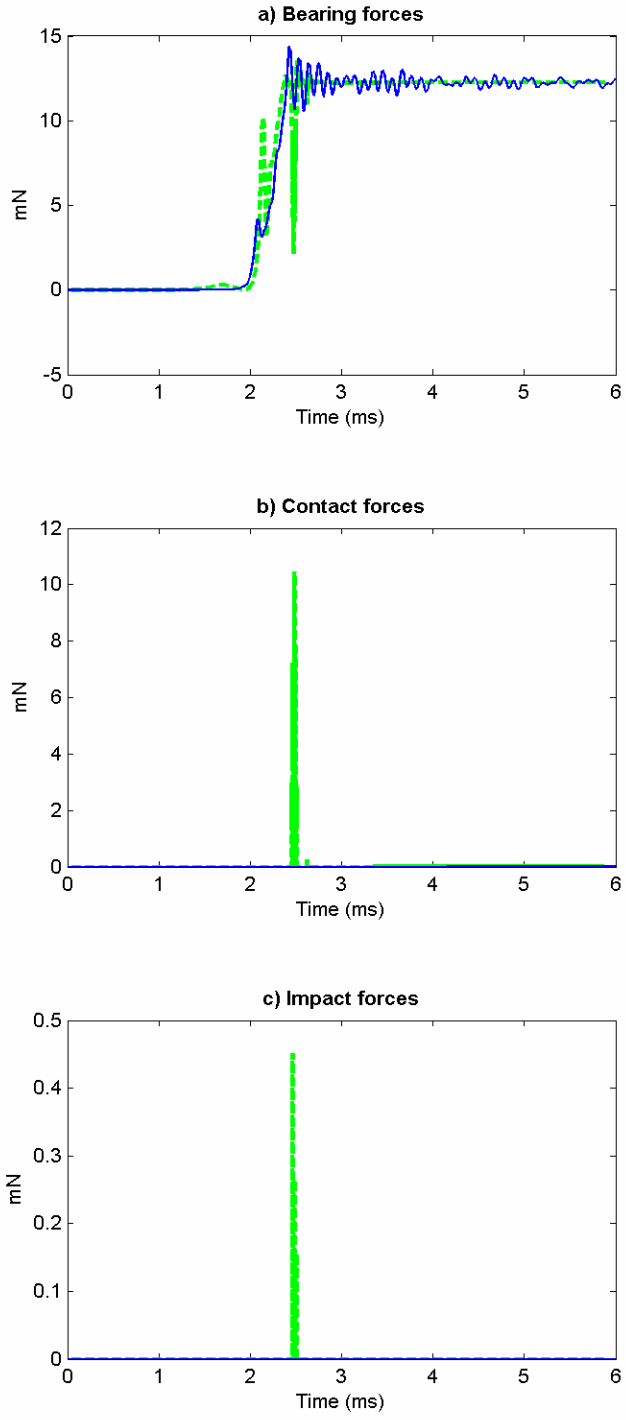

Fig 19. Force history comparison during the loading process (66.7 mm/s)

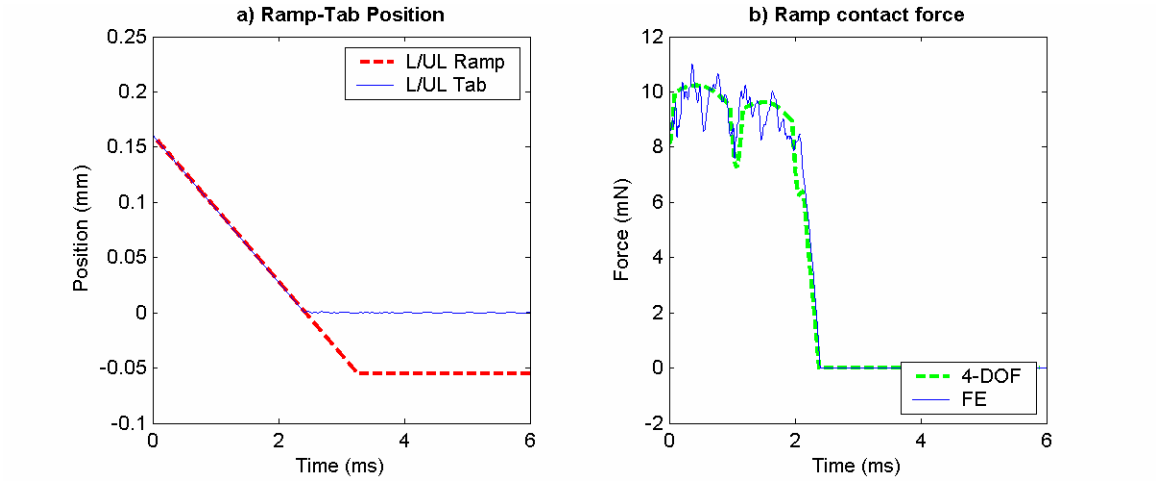

Fig 20. Ramp-tab position and ramp contact force during the loading process (66.7 mm/s)

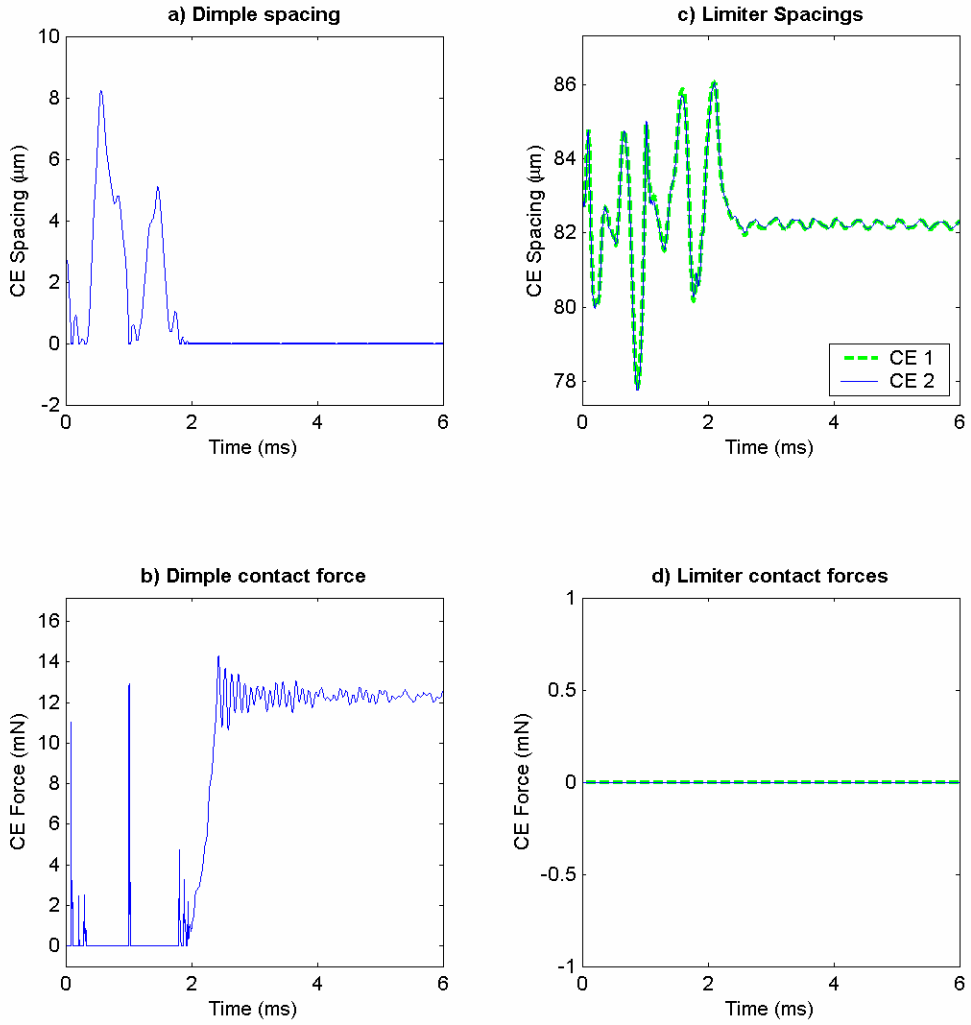

Fig 21. Dimple and limiter contact status during the loading process (66.7 mm/s)

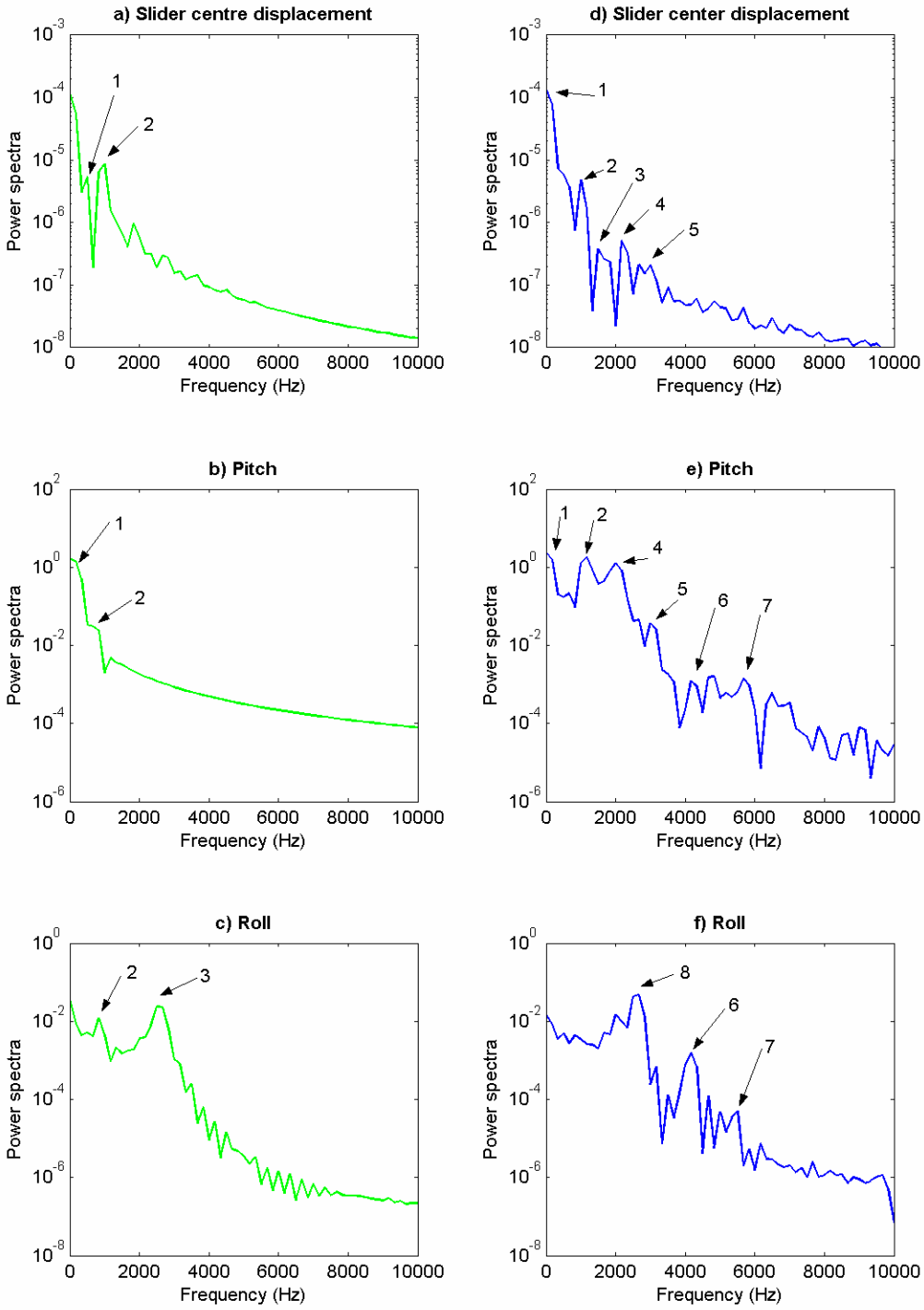

Fig 22. Frequency spectra of a typical L/UL process for 4-DOF (a, b, c) and FE based (d, e, f) simulators